

The Signal Horizon: Local Blindness and the Contraction of Pauli-Weight Spectra in Noisy Quantum Encodings

AIT HADDOU Marwan *,

¹*Independent Researcher*

(Dated: February 17, 2026)

The performance of quantum classifiers is typically analyzed either through global state distinguishability or through the trainability of variational models. Here we study a more operational question: how much class information remains accessible under locality-constrained measurements in the presence of noise.

We formulate binary quantum classification as constrained quantum state discrimination and introduce a locality-restricted distinguishability measure that quantifies the maximum bias achievable by observables acting on at most k subsystems. For n -qubit systems subject to independent depolarizing noise, we show that locally accessible signal is governed by a Pauli-weight-dependent contraction mechanism. This motivates a computable predictor, the k -local Pauli-accessible amplitude $A_k(p)$, which lower bounds the optimal k -local classification advantage.

Numerical experiments on four-qubit encodings demonstrate quantitative agreement between empirical accuracy and the prediction $\frac{1}{2} + \frac{1}{4}A_k(p)$ across noise levels. In entangling encodings where class information is distributed across higher Pauli weights, we observe regimes in which global trace distance remains finite while locally accessible signal collapses to the statistical resolution scale. This identifies an operational breakdown threshold at which k -local classifiers become indistinguishable from random guessing despite persistent global distinguishability.

Our results isolate measurement locality and noise-induced correlation-order contraction as independent limitations on quantum classification performance. The framework provides a measurement-theoretic constraint that complements existing analyses of trainability and kernel expressivity in quantum machine learning.

I. INTRODUCTION

Quantum machine learning (QML) has been proposed as a route toward information processing that exploits uniquely quantum resources such as superposition, entanglement, and high-dimensional Hilbert spaces. Early theoretical and experimental work suggested that quantum feature maps and variational circuits could represent complex data in ways that are difficult to emulate classically, motivating a wide range of algorithms for classification, regression, and generative modeling [1–3]. As hardware has transitioned to noisy intermediate-scale quantum (NISQ) devices with tens to hundreds of qubits, attention has increasingly shifted from idealized algorithmic advantages to the more fundamental question of what information quantum systems can reliably encode, preserve, and reveal under realistic noise and measurement constraints [4, 5]. In this regime, performance is limited not only by computational power but also by the physical accessibility of quantum information.

A large body of work has therefore focused on the limitations of variational quantum algorithms, particularly the phenomenon of barren plateaus, in which gradients of typical cost functions vanish exponentially with system size for broad classes of deep or highly entangling ansätze [6–8]. In parallel, quantum kernel methods have been developed to analyze the expressivity of quantum feature maps through their induced Gram matrices and

reproducing kernel Hilbert spaces, providing insight into generalization, trainability, and classical post-processing [3, 9, 10]. Together, these approaches have framed much of the current understanding of when QML models are likely to succeed or fail.

Despite this progress, existing frameworks primarily assess performance at the level of optimization dynamics or classical learning theory, rather than at the level of physical measurability. Barren plateau analyses implicitly assume that the relevant class information exists in the quantum state but is difficult to optimize, while kernel-based approaches typically assume that the encoded information is fully accessible to a chosen measurement scheme [11]. Neither perspective directly addresses a more primitive question: whether class-dependent information remains operationally extractable by realistic, locality-constrained measurements after noise has acted on the system. This creates a gap between what quantum states may contain in principle and what can actually be detected in practice, especially in NISQ architectures with limited measurement capabilities [12, 13].

In this work, we introduce a measurement-first framework for QML based on the concept of a *Signal Horizon*: a noise-locality boundary beyond which class information may persist globally but becomes inaccessible to any observer restricted to k -local measurements. We formalize this idea using the locality-restricted distinguishability seminorm $\|\cdot\|_{\text{LO}(k)}$, rooted in constrained quantum hypothesis testing and local state discrimination [11, 13, 14]. We further define a computable Pauli-accessible proxy $A_k(p)$, which predicts the maxi-

* aithaddou.marwan@outlook.com; Corresponding author.

imum achievable classification accuracy for any single k -local Pauli measurement under independent depolarizing noise. Crucially, this bound is independent of ansatz, training procedure, or optimizer, and instead depends only on the encoded states, the noise model, and measurement locality. Our central claim is that $A_k(p)$ sets a fundamental, training-independent ceiling on operational performance in realistic QML settings.

The paper proceeds as follows. In Sec. II, we develop the theoretical framework linking constrained quantum hypothesis testing [11, 15], Pauli-weight spectra [16, 17], and depolarizing noise to the Signal Horizon criterion; we further provide a formal comparison between this measurement-theoretic perspective and established QML paradigms such as barren plateaus [6, 7] and quantum kernels [3, 9]. In Sec. III, we describe the numerical methodology, detailing the product and entangling encodings, the noise implementation, and the split-sample protocol used to estimate $A_k(p)$ without maximization bias. In Sec. IV, we present numerical results that validate the predicted accuracy bound and demonstrate the emergence of the Signal Horizon. Finally, in Secs. V and ??, we discuss the implications of our findings for the design of robust NISQ-era quantum machine learning systems [4, 5].

II. THEORETICAL FRAMEWORK

A. Binary quantum classification as constrained state discrimination

We consider supervised binary classification with labels $y \in \{+1, -1\}$ and class-conditional states $\rho_+, \rho_- \in \mathcal{D}(\mathcal{H})$, assumed equiprobable unless stated otherwise. Define the *signal operator*

$$\Delta\rho := \rho_+ - \rho_-. \quad (1)$$

A measurement-based classifier is specified by a Hermitian observable M with operator norm constraint $\|M\|_\infty \leq 1$, together with the decision rule $\hat{y} = \text{sign}(\text{Tr}(M\rho))$. For balanced priors, the success probability (accuracy) is

$$\text{Acc}(M) = \frac{1}{2} + \frac{1}{4} \text{Tr}(M\Delta\rho). \quad (2)$$

This is the standard reduction of binary hypothesis testing to an affine functional of $\Delta\rho$ under the choice of a two-outcome measurement [11, 15, 18].

Theorem 1 (Helstrom optimum for unconstrained measurements). *Let $\|M\|_\infty \leq 1$. Then*

$$\sup_{\|M\|_\infty \leq 1} \text{Tr}(M\Delta\rho) = \|\Delta\rho\|_1, \quad \text{Acc}_{\text{opt}} = \frac{1}{2} + \frac{1}{4} \|\Delta\rho\|_1. \quad (3)$$

Proof. The duality between trace norm and operator norm gives $\|\Delta\rho\|_1 = \sup_{\|M\|_\infty \leq 1} \text{Tr}(M\Delta\rho)$, achieved by $M = \text{sign}(\Delta\rho)$. Substituting into (2) yields (3) [11, 15, 18]. \square

B. Locality-restricted distinguishability

In realistic architectures, accessible measurements are restricted in locality. Let \mathcal{M}_k denote the set of Hermitian observables acting nontrivially on at most k subsystems (implicitly with $\|M\|_\infty \leq 1$). We define the *locality-restricted distinguishability seminorm*

Definition 1 (LO(k) seminorm). *For $\Delta\rho$ on n qubits, define*

$$\|\Delta\rho\|_{\text{LO}(k)} := \sup_{M \in \mathcal{M}_k} |\text{Tr}(M\Delta\rho)|. \quad (4)$$

Lemma 1 (Optimal k -local accuracy as constrained testing). *For balanced priors, the maximum achievable accuracy using observables in \mathcal{M}_k is*

$$\text{Acc}_k = \frac{1}{2} + \frac{1}{4} \|\Delta\rho\|_{\text{LO}(k)}. \quad (5)$$

Proof. By (2), maximizing $\text{Acc}(M)$ over $M \in \mathcal{M}_k$ is equivalent to maximizing $\text{Tr}(M\Delta\rho)$ over the same set, up to an absolute value from label-swapping. This yields (5) by Definition 1 [11]. \square

C. Pauli decomposition and correlation order

For n qubits, the Pauli strings \mathcal{P}_n form an orthonormal operator basis (Hilbert–Schmidt inner product) [16, 17]. Accordingly,

$$\Delta\rho = \sum_{P \in \mathcal{P}_n} c_P P, \quad c_P = 2^{-n} \text{Tr}(P\Delta\rho). \quad (6)$$

The *Pauli weight* $w(P)$ is the number of non-identity tensor factors in P . We define the weight-resolved magnitude spectrum

$$W_\ell(\Delta\rho) := \sum_{w(P)=\ell} |c_P|. \quad (7)$$

The profile $\{W_\ell\}_{\ell=0}^n$ quantifies how class-dependent information is distributed across correlation orders.

D. Independent depolarizing noise as Pauli-weight contraction

We model noise by independent single-qubit depolarizing channels,

$$\mathcal{D}_p(\rho) = (1-p)\rho + \frac{p}{3} \sum_{\alpha \in \{X, Y, Z\}} \sigma_\alpha \rho \sigma_\alpha, \quad \mathcal{N}_p := \mathcal{D}_p^{\otimes n}. \quad (8)$$

This parametrization yields the familiar diagonal action on Pauli operators:

$$\mathcal{D}_p(P) = \lambda(p)P \text{ for single-qubit Pauli } P \neq I, \quad \lambda(p) = 1 - \frac{4p}{A_k(p)} \leq 2^n \max_{\ell \leq k} \lambda(p)^\ell \max_{w(P)=\ell} |c_P| \leq 2^n \max_{\ell \leq k} \lambda(p)^\ell W_\ell(\Delta\rho). \quad (9)$$

and therefore

$$\mathcal{N}_p(P) = \lambda(p)^{w(P)} P \quad \text{for } P \in \mathcal{P}_n. \quad (10)$$

See, e.g., [11, 17].

Applying \mathcal{N}_p to the signal operator gives

$$\mathcal{N}_p(\Delta\rho) = \sum_{P \in \mathcal{P}_n} c_P \lambda(p)^{w(P)} P. \quad (11)$$

E. Pauli-accessible local signal and a computable predictor

When measurements are further restricted to *Pauli* observables of weight at most k , the corresponding accessible amplitude becomes explicit.

Definition 2 (k -local Pauli-accessible amplitude). *Define*

$$A_k(p) := \max_{\substack{P \in \mathcal{P}_n \\ w(P) \leq k}} \left| \text{Tr}(P \mathcal{N}_p(\Delta\rho)) \right| = \max_{\substack{P \in \mathcal{P}_n \\ w(P) \leq k}} \left| 2^n c_P \right| \lambda(p)^{w(P)}. \quad (12)$$

Remark 1 (Normalization). *If one uses the coefficient convention $c_P = 2^{-n} \text{Tr}(P \Delta\rho)$ as in (6), then $\text{Tr}(P \mathcal{N}_p(\Delta\rho)) = 2^n c_P \lambda(p)^{w(P)}$. If instead one defines $\tilde{c}_P := \text{Tr}(P \Delta\rho)$, then $A_k(p) = \max_{w(P) \leq k} |\tilde{c}_P| \lambda(p)^{w(P)}$. All operational statements below hold under either convention, provided the same convention is used consistently in the accuracy mapping (2).*

Lemma 2 (Pauli restriction lower-bounds $\text{LO}(k)$ distinguishability). *Let \mathcal{M}_k contain all weight- $\leq k$ Pauli observables (with $\|P\|_\infty = 1$). Then*

$$\|\mathcal{N}_p(\Delta\rho)\|_{\text{LO}(k)} \geq A_k(p). \quad (13)$$

Proof. The supremum in (4) is taken over a set that includes the weight- $\leq k$ Pauli observables. Therefore it is at least as large as the maximum over that subset, which is $A_k(p)$ by Definition 2. \square

F. Accuracy bounds under locality and noise (Signal Horizon criterion)

Combining Lemma 1 with Lemma 2 yields an operational performance bound for Pauli-local classifiers:

$$\text{Acc}_k(p) = \frac{1}{2} + \frac{1}{4} \|\mathcal{N}_p(\Delta\rho)\|_{\text{LO}(k)} \geq \frac{1}{2} + \frac{1}{4} A_k(p). \quad (14)$$

Moreover, $A_k(p)$ can be upper bounded using the weight spectrum (7). For any P with $w(P) = \ell \leq k$, one has $|\text{Tr}(P \mathcal{N}_p(\Delta\rho))| \leq 2^n |c_P| \lambda(p)^\ell$, so

$$\frac{4p}{A_k(p)} \leq 2^n \max_{\ell \leq k} \lambda(p)^\ell \max_{w(P)=\ell} |c_P| \leq 2^n \max_{\ell \leq k} \lambda(p)^\ell W_\ell(\Delta\rho). \quad (15)$$

This makes explicit the interplay between correlation order (weight) and noise-induced contraction.

Definition 3 (Operational breakdown threshold). *Let ϵ denote an experimentally resolvable bias scale. Define p^* implicitly by*

$$A_k(p^*) \approx \epsilon. \quad (16)$$

Remark 2 (Signal Horizon interpretation). *For $p > p^*$, the Pauli-accessible advantage in (14) is at most $O(\epsilon)$, hence observed accuracy approaches $1/2$ at the scale of experimental resolution, even when global distinguishability persists (i.e., $\|\mathcal{N}_p(\Delta\rho)\|_1 > 0$). This identifies a regime where class information remains present in the global state but is inaccessible under locality-constrained measurements.*

G. Statistical resolution and sample complexity

With N repetitions of a ± 1 -valued Pauli measurement, empirical averages obey concentration bounds. In particular, Hoeffding's inequality implies that, with confidence $1 - \delta$,

$$|\hat{\mu}_P - \mu_P| \lesssim \sqrt{\frac{\log(2/\delta)}{2N}}, \quad \mu_P := \text{Tr}(P \mathcal{N}_p(\Delta\rho)). \quad (17)$$

Consequently, resolving a bias of order $A_k(p)$ requires

$$A_k(p) \gtrsim \sqrt{\frac{\log(2/\delta)}{2N}} \iff N \gtrsim \frac{\log(2/\delta)}{2 A_k(p)^2}, \quad (18)$$

up to constants [19].

H. Relation to Fisher information

Consider the parametric family

$$\rho_\theta := \frac{1}{2}(\rho_+ + \rho_-) + \frac{\theta}{2} \Delta\rho. \quad (19)$$

For a two-outcome measurement associated to observable M (with $\|M\|_\infty \leq 1$), the classical Fisher information at $\theta = 0$ scales as

$$F_M(0) \propto (\text{Tr}(M \Delta\rho))^2, \quad (20)$$

under standard regularity assumptions [20, 21]. Restricting to weight- $\leq k$ Pauli observables and including \mathcal{N}_p yields

$$F_k(p) \sim A_k(p)^2, \quad (21)$$

so suppression of $A_k(p)$ corresponds to collapse of locally accessible classical Fisher information.

I. Relation to existing paradigms in quantum machine learning

We situate the present framework relative to two dominant QML analyses: variational trainability (barren plateaus) and kernel-based learning.

1. Distinction from barren plateau analyses

Barren plateau results characterize the optimization landscape of parameterized quantum circuits by showing that gradients of typical cost functions concentrate near zero for broad classes of ansätze, often with unfavorable scaling in system size [6, 7]. These analyses concern the behavior of quantities of the form

$$\partial_\theta \langle O(\theta) \rangle, \quad (22)$$

for a chosen variational model and cost observable $O(\theta)$.

By contrast, the present framework addresses a logically prior question: given an encoding, a noise model, and a measurement locality constraint, how much class information remains *operationally accessible*? This is captured by $\|\mathcal{N}_p(\Delta\rho)\|_{\text{LO}(k)}$ and its Pauli-accessible proxy $A_k(p)$, which depend only on the encoded states and the channel, not on an optimizer or training dynamics. Accordingly, vanishing gradients do not imply $A_k(p) \approx 0$, and conversely $A_k(p) \approx 0$ implies that no k -local measurement can extract a statistically resolvable advantage even under ideal optimization.

2. Relation to quantum kernel methods

Quantum kernel approaches analyze the Gram matrix

$$K_{ij} := \text{Tr}(\rho(x_i)\rho(x_j)), \quad (23)$$

and study expressivity and generalization via properties of the induced feature map and classical post-processing [3, 9]. Our framework does not assume a kernel representation. Instead, it supplies a measurement-level constraint on the achievable discrimination under locality and noise:

$$\text{Acc}_k(p) = \frac{1}{2} + \frac{1}{4} \|\mathcal{N}_p(\Delta\rho)\|_{\text{LO}(k)} \geq \frac{1}{2} + \frac{1}{4} A_k(p). \quad (24)$$

Thus, even when a global feature map yields strong separation in kernel space, the operational performance under k -local measurements is limited by the locally accessible signal amplitude.

3. Complementarity

Barren plateaus, kernels, and the Signal Horizon address different layers of the learning pipeline: (i) encoding geometry (Pauli-weight spectrum), (ii) physical noise

contraction, (iii) measurement accessibility, (iv) training dynamics, and (v) classical post-processing. The present contribution is a measurement-theoretic constraint that any variational or kernel-based model must respect in the presence of locality constraints and noise in the NISQ regime [4].

III. METHOD

Our numerical experiments instantiate the objects introduced in Sec. II in a fully explicit simulation setting. In particular, we evaluate the noisy signal operator $\mathcal{N}_p(\Delta\rho)$ [Eq. (11)], compute its global trace norm $\|\mathcal{N}_p(\Delta\rho)\|_1$, and estimate the Pauli-restricted k -local amplitude $A_k(p)$ [Def. 2] using direct Monte Carlo sampling. All quantities are extracted from state-preparation and measurement circuits implemented in a density-matrix simulator with finite sampling.

A. State preparation and encodings

We consider two encoding families that realize distinct Pauli-weight structures.

a. Product encoding. For the baseline regime, we prepare separable states

$$\rho_+ = |+\rangle\langle+|^{\otimes n}, \quad \rho_- = |-\rangle\langle-|^{\otimes n}. \quad (25)$$

In this case, the signal operator $\Delta\rho = \rho_+ - \rho_-$ has support predominantly in weight-1 Pauli sectors. This encoding provides a controlled reference where locality constraints are not expected to significantly reduce distinguishability.

b. Entangling encoding. To generate higher-weight correlations, we prepare

$$|\psi_+(\theta)\rangle = U(\theta)|0\rangle^{\otimes n}, \quad |\psi_-(\theta)\rangle = Z_1|\psi_+(\theta)\rangle, \quad (26)$$

where $U(\theta)$ consists of: (i) a layer of Hadamards, (ii) local $R_Z(\theta)$ rotations, (iii) a ring of nearest-neighbor CNOT gates.

This circuit spreads class-dependent information across multiple Pauli weights $W_\ell(\Delta\rho)$ [Eq. (7)], thereby producing a regime in which locality and noise interact nontrivially.

Unless otherwise stated, the main text focuses on $n = 4$ qubits, where both global and local quantities can be evaluated exactly within the simulator. Larger system sizes are treated in the Appendix using locality-restricted quantities only.

B. Noise model

Noise is modeled as independent single-qubit depolarizing channels,

$$\mathcal{D}_p(\rho) = (1-p)\rho + \frac{p}{3} \sum_{\alpha \in \{X,Y,Z\}} \sigma_\alpha \rho \sigma_\alpha, \quad \mathcal{N}_p = \mathcal{D}_p^{\otimes n}. \quad (27)$$

Operationally, the channel is inserted after state preparation in the circuit. In the Pauli basis, this realizes the diagonal contraction

$$\mathcal{N}_p(P) = \lambda(p)^{w(P)} P, \quad \lambda(p) = 1 - \frac{4p}{3}, \quad (28)$$

so that higher-weight correlations decay faster than low-weight ones.

C. Global distinguishability

For $n = 4$, we compute the global trace norm exactly from the simulated density matrices:

$$\|\mathcal{N}_p(\Delta\rho)\|_1 = \|\rho_+(p) - \rho_-(p)\|_1, \quad (29)$$

where $\rho_\pm(p)$ are obtained directly from the density-matrix simulator. Singular values are computed numerically, and their absolute sum yields the trace norm.

This quantity serves as a reference measure of globally available class information.

D. Enumeration of k -local Pauli observables

For each locality parameter k , we explicitly enumerate all Pauli strings P with weight $w(P) \leq k$. For $n = 4$, this enumeration is exact and computationally inexpensive.

For each Pauli string, we estimate

$$\mu_P(p) = \text{Tr}(P \mathcal{N}_p(\Delta\rho)) = \langle P \rangle_{\rho_+(p)} - \langle P \rangle_{\rho_-(p)}. \quad (30)$$

Expectation values are obtained via repeated projective measurements of P in the simulator.

E. Split-sample estimation of $A_k(p)$

To avoid maximization bias, we employ a split-shot protocol consistent with the implementation in the code.

For each P and noise level p :

1. N_{search} shots are used to estimate μ_P^{search} .
2. The maximizing observable is selected:

$$P^* = \arg \max_{w(P) \leq k} |\mu_P^{\text{search}}|.$$

3. N_{eval} fresh shots are used to estimate

$$\hat{A}_k(p) = |\mu_{P^*}^{\text{eval}}|.$$

The total shot budget is $N = N_{\text{search}} + N_{\text{eval}}$ per Pauli string. This procedure matches the QNode implementation and ensures that the reported $\hat{A}_k(p)$ is not inflated by reuse of search data.

F. Empirical classification accuracy

Given P^* , the classifier is a single Pauli measurement with decision rule determined by the measurement outcome sign.

From the evaluation shots, we estimate

$$\widehat{\text{Acc}}_k(p) = \frac{1}{2} [\mathbb{P}(+1|\rho_+) + \mathbb{P}(-1|\rho_-)]. \quad (31)$$

We compare this empirical accuracy to the theoretical prediction

$$\frac{1}{2} + \frac{1}{4} A_k(p), \quad (32)$$

derived in Sec. II. Agreement between these quantities constitutes a direct operational test of the framework.

G. Statistical resolution and operational threshold

Each expectation value is estimated from finite samples. For N_{eval} shots, the typical statistical fluctuation scale is

$$\epsilon \sim \frac{1}{\sqrt{N_{\text{eval}}}}, \quad (33)$$

consistent with Hoeffding-type concentration bounds.

We therefore define the operational threshold p^* as the noise level at which

$$A_k(p^*) \approx \epsilon. \quad (34)$$

Beyond this point, a k -local Pauli classifier becomes statistically indistinguishable from random guessing at the given shot budget, even if $\|\mathcal{N}_p(\Delta\rho)\|_1$ remains nonzero.

H. Reported quantities

For each encoding and each $k \in \{1, 2, 3\}$, we report:

- the global trace norm (for $n = 4$),
- the split-sample estimate $\hat{A}_k(p)$,
- empirical accuracy $\widehat{\text{Acc}}_k(p)$,
- the optimal Pauli weight $w(P^*)$,
- and the statistical resolution scale ϵ .

These observables correspond directly to quantities computed in the simulation code and provide an explicit bridge between the abstract definitions of Sec. II and experimentally measurable performance.

IV. RESULTS

We now present the numerical results obtained using the procedures described in Sec. III. For $n = 4$ qubits, both the global trace norm $\|\mathcal{N}_p(\Delta\rho)\|_1$ and the locality-restricted quantity $A_k(p)$ are evaluated under independent depolarizing noise. The latter is estimated using the split-sample protocol detailed in Sec. III, with $N_{\text{search}} = N_{\text{eval}} = 2 \times 10^4$ shots per Pauli string. This yields a statistical resolution scale $\epsilon \sim 1/\sqrt{N_{\text{eval}}}$, which serves as the operational threshold for resolving nonzero local signal.

Our objective is twofold. First, we test whether the empirical classification accuracy is quantitatively captured by the predictor $\frac{1}{2} + \frac{1}{4}A_k(p)$. Second, we examine how the globally available distinguishability $\|\mathcal{N}_p(\Delta\rho)\|_1$ compares to the locally accessible amplitude $A_k(p)$ as noise increases.

We consider two encoding families introduced in Sec. III: (i) a separable product-state encoding that concentrates signal at low Pauli weight, and (ii) a structured entangling encoding that distributes class-dependent information across multiple correlation orders. These complementary regimes allow us to probe both the trivial and genuinely locality-constrained limits of the framework.

A. Product encoding: low-weight signal regime

Figure 1 summarizes the results for the product encoding. In this setting, the signal operator $\Delta\rho$ is supported predominantly in weight-1 Pauli sectors.

Several features are evident.

First, the global trace norm and $A_k(p)$ are nearly coincident for all k . The accessible fraction $A_k/\|\Delta\rho\|_1$ remains close to unity throughout the noise range. The gap $\|\Delta\rho\|_1 - A_k$ is small and vanishes as $p \rightarrow 0$ and as p approaches complete depolarization.

Second, the optimal observable weight remains $w(P^*) = 1$ across noise levels. Increasing k does not significantly change the accessible amplitude.

Third, the empirical accuracy agrees with the theoretical prediction

$$\text{Acc}_k(p) = \frac{1}{2} + \frac{1}{4}A_k(p), \quad (35)$$

within statistical uncertainty for all k .

These results confirm that when class information is concentrated in low-weight sectors, locality constraints do not substantially limit operational distinguishability. In this regime, the Signal Horizon mechanism is inactive: accessibility is governed primarily by noise contraction rather than measurement locality.

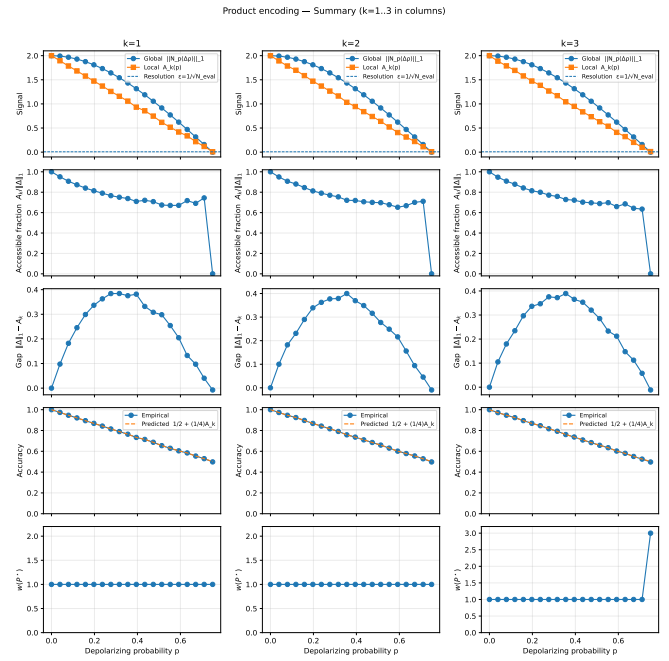


FIG. 1. Product encoding ($n = 4$). (Top row) Global trace norm $\|\mathcal{N}_p(\Delta\rho)\|_1$ and local amplitude $A_k(p)$ for $k = 1, 2, 3$. (Middle row) Accessible fraction $A_k/\|\Delta\rho\|_1$ and gap $\|\Delta\rho\|_1 - A_k$. (Bottom row) Empirical classification accuracy and theoretical prediction $\frac{1}{2} + \frac{1}{4}A_k(p)$, together with optimal Pauli weight $w(P^*)$.

B. Entangling encoding: separation of global and accessible information

We now turn to the structured entangling encoding, in which the signal operator exhibits significant support in higher Pauli weights.

The behavior differs qualitatively from the product case (Fig. 2).

At low noise, the global trace norm $\|\mathcal{N}_p(\Delta\rho)\|_1$ is substantially larger than $A_1(p)$. The accessible fraction $A_1/\|\Delta\rho\|_1$ is approximately 0.4–0.5 at $p = 0$, indicating that a significant portion of class information resides in correlations inaccessible to 1-local measurements.

The gap

$$\Delta(p) := \|\mathcal{N}_p(\Delta\rho)\|_1 - A_1(p) \quad (36)$$

is maximal near $p = 0$ and decreases monotonically with noise. This reflects the weight-dependent contraction $\lambda(p)^{w(P)}$, which suppresses higher-weight components more rapidly. As p increases, the remaining signal becomes increasingly concentrated in low-weight sectors, reducing the global-local discrepancy before eventual collapse.

Increasing the locality parameter systematically reduces the separation. For $k = 2$, the accessible amplitude is closer to the global trace norm at all noise levels, and for $k = 3$ the discrepancy is further diminished.

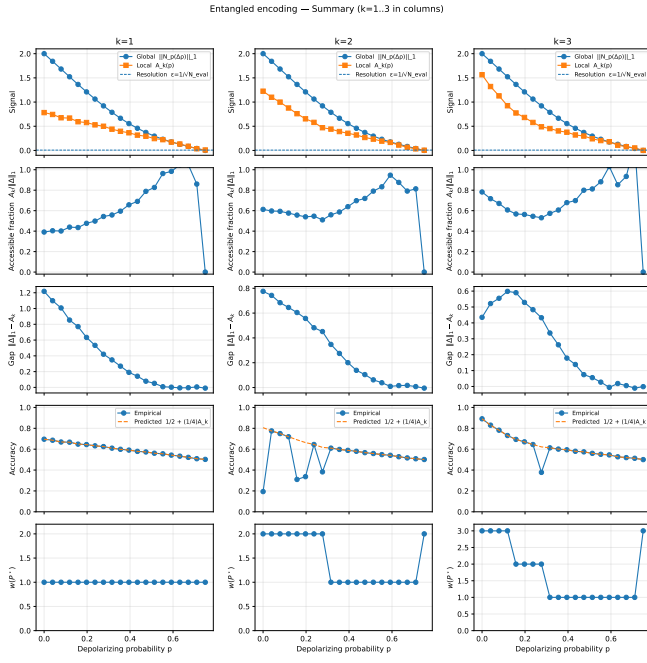


FIG. 2. Entangling encoding ($n = 4$). (Top row) Global trace norm and local amplitude $A_k(p)$. (Middle row) Accessible fraction and global-local gap. (Bottom row) Empirical versus predicted accuracy and optimal Pauli weight flow under noise.

This monotonic behavior is consistent with the definition of the $LO(k)$ seminorm and its Pauli-restricted lower bound.

The optimal Pauli weight $w(P^*)$ exhibits a clear downward flow under noise. At low p , the maximizing observable lies in higher-weight sectors (e.g., $w = 2$ or 3 depending on k). As noise increases, the optimal weight transitions to lower values. This behavior directly visualizes the Pauli-weight contraction mechanism described in Sec. II D.

Finally, empirical classification accuracy agrees quantitatively with the theoretical prediction $\frac{1}{2} + \frac{1}{4}A_k(p)$ across all tested values of k and p , including in the entangled regime where global and local distinguishability differ significantly.

C. Operational interpretation

Taken together, the results establish three observations for the tested system size:

1. Global distinguishability, as measured by the trace norm, does not by itself determine achievable classification accuracy under locality constraints.
2. The Pauli-accessible amplitude $A_k(p)$ accurately predicts operational performance of k -local Pauli classifiers across noise levels.

3. Independent depolarizing noise induces a weight-dependent contraction that can transiently increase the accessible fraction by preferentially suppressing higher-order correlations.

We emphasize that these findings do not claim fundamental limits beyond the modeled setting. The results demonstrate, for the considered encodings and noise model, that locality constraints can generate a measurable separation between globally present and operationally accessible class information, and that this separation is quantitatively captured by the proposed framework.

V. DISCUSSION

Summary of main findings

The numerical experiments directly tested the central prediction of the Signal Horizon framework: that the best achievable k -local Pauli classification accuracy under noise is controlled by the locally accessible amplitude $A_k(p)$ rather than by the global trace norm $\|\mathcal{N}_p(\Delta\rho)\|_1$. Across both encoding families, the empirical accuracies were found to agree quantitatively with the predictor

$$Acc_k(p) \approx \frac{1}{2} + \frac{1}{4}A_k(p), \quad (37)$$

within statistical uncertainty.

In the product-state encoding, where the signal is concentrated at low Pauli weight, $A_k(p)$ tracked the global trace norm closely for small k , and no substantial separation between global and local distinguishability emerged. In contrast, in the structured entangling encoding, a clear gap developed between $\|\mathcal{N}_p(\Delta\rho)\|_1$ and $A_k(p)$ at small k , demonstrating that globally preserved information may become operationally inaccessible under locality constraints. These observations are consistent with the structural mechanism articulated in Sec. II.

Interpretation and relation to existing analyses

Our findings are naturally situated within the broader literature on *state discrimination under restricted measurements*, where the Helstrom trace distance is replaced by a measurement-dependent seminorm that captures the maximum achievable bias over an allowed measurement family [22]. A systematic formulation of this viewpoint—defining distinguishability norms/seminorms induced by restricted POVM classes and using them to quantify the loss relative to global discrimination—was developed in the context of quantum data hiding and constrained hypothesis testing [23]. In that line of work, pairs of states can be constructed whose global trace distance is large while the bias achievable under restricted

measurements (e.g., LOCC) is parametrically small, implying that information is present globally but inaccessible to the restricted observer. Closely related quantitative bounds on local discrimination norms in multipartite settings were later obtained, including dimension- and party-dependent comparisons between global and local distinguishability [24]. More recently, the size of the maximal separation between global and local (LO/LOCC) distinguishability has been sharpened via explicit upper and lower bounds on data-hiding ratios [25], and optimization of data-hiding constructions continues to be an active topic [26].

Our contribution differs in emphasis and in the constraints of interest. Rather than constructing adversarial data-hiding pairs, we studied *noise-filtered accessibility* for structured encodings relevant to quantum machine learning, with the restriction set by k -local Pauli measurements and with performance assessed through an explicit classification protocol. The central empirical observation—the coexistence of nonzero global distinguishability $\|\mathcal{N}_p(\Delta\rho)\|_1$ with strongly suppressed locally accessible amplitude $A_k(p)$ in the entangling encoding—matches the qualitative “global-versus-restricted” separation highlighted in data hiding [23–25], but arises here from a concrete mechanism: independent depolarizing noise contracts Pauli sectors by $\lambda(p)^{w(P)}$, preferentially erasing high-weight correlations that dominate $\Delta\rho$ for entangling feature maps. This produces an *operational* transition in attainable accuracy at fixed shot budget when $A_k(p)$ falls below the statistical resolution scale, even though global trace distance remains finite.

A complementary connection is to recent work defining information measures *after optimization over restricted measurement families*. For example, locally measured Rényi divergences formalize the idea of replacing global distinguishability by divergences induced by local measurements, with applications to operational tasks under measurement restrictions [27]. In our setting, the quantity $\|\mathcal{N}_p(\Delta\rho)\|_{\text{LO}(k)}$ plays an analogous operational role for binary discrimination, while $A_k(p)$ provides an experimentally direct, Pauli-restricted proxy that is computable by explicit enumeration for small k and can be estimated with finite sampling.

Finally, these measurement-theoretic constraints are logically distinct from dominant QML explanations based on optimization landscapes (barren plateaus) or feature-space separation (kernels). Barren plateaus diagnose trainability through gradient concentration for specific variational objectives, whereas our results address the *existence of a resolvable measurement bias* under locality and noise, independent of any optimizer. Kernel analyses quantify similarity through global overlaps or induced Gram matrices, but do not by themselves guarantee that the information driving separation is accessible under the measurement constraints imposed by hardware. In this sense, locality-restricted distinguishability complements existing analyses by isolating a measurement-accessibility layer that any training-based

or kernel-based pipeline must ultimately confront in the presence of noise and locality constraints.

Limitations

Several limitations should be acknowledged. First, the primary validation was performed at $n = 4$ qubits, where exact global trace norms are computationally tractable. Although additional simulations at larger n confirm the scaling behavior of $A_k(p)$, full global-local comparisons were restricted to small system sizes. Second, the experiments focused on independent depolarizing noise, which acts diagonally in the Pauli basis. Correlated or non-Pauli noise channels may alter quantitative contraction rates. Third, the classifier was restricted to single Pauli observables; while this isolates the operational meaning of $A_k(p)$, more general k -local observables could slightly increase achievable accuracy, though they remain bounded by $\|\cdot\|_{\text{LO}(k)}$.

Finally, the encodings studied here are structured but stylized. Realistic QML feature maps may exhibit more complex Pauli spectra, and empirical datasets may introduce additional classical sampling noise not modeled in this controlled setting.

Implications

The results provide an operational interpretation of locality-restricted distinguishability in noisy quantum classification. They suggest that performance degradation in near-term devices can arise not only from optimization pathologies but from fundamental measurement-accessibility constraints. In practical terms, increasing circuit depth or entanglement does not guarantee improved classification accuracy if the resulting signal is concentrated in high-weight Pauli sectors that are rapidly suppressed by noise.

More broadly, the framework separates three distinct layers of analysis: (i) encoding geometry (Pauli-weight spectrum), (ii) noise-induced contraction, and (iii) measurement accessibility. This separation clarifies how physical noise and architectural constraints combine to determine observable learning performance.

Future directions

Several extensions are natural. Analytically characterizing $A_k(p)$ for broader families of encodings would clarify scaling behavior beyond small n . Incorporating correlated noise models could test the robustness of the weight-contraction picture. Extending the analysis to multi-observable or adaptive measurement strategies would bound the gap between Pauli-restricted and fully $\text{LO}(k)$ -optimal discrimination. Finally, connecting locality-restricted distinguishability to generalization

theory in quantum kernel models may clarify how operational accessibility interacts with statistical learning bounds.

Conclusion

The numerical evidence supports a precise and limited claim: in the studied settings, the locally accessible amplitude $A_k(p)$ accurately predicts the maximum achievable accuracy of k -local Pauli classifiers under depolarizing noise, and this quantity can decay substantially faster than the global trace norm. Consequently, global distinguishability does not guarantee operationally acces-

sible class information under locality constraints. This measurement-theoretic limitation provides a complementary perspective to existing analyses of trainability and expressivity in quantum machine learning.

ACKNOWLEDGMENTS

The author expresses sincere gratitude to Professor Mohammed Bennai  for insightful discussions and guidance throughout the development of this work. The author also acknowledges the use of generative AI tools for assistance in the structuring and drafting of the manuscript.

[1] M. Schuld, I. Sinayskiy, and F. Petruccione, *Contemporary Physics* **56**, 172 (2015).

[2] J. Biamonte, P. Wittek, N. Pancotti, P. Rebentrost, N. Wiebe, and S. Lloyd, *Nature* **549**, 195 (2017).

[3] V. Havlíček, A. D. Córcoles, K. Temme, A. W. Harrow, A. Kandala, J. M. Chow, and J. M. Gambetta, *Nature* **567**, 209 (2019).

[4] J. Preskill, *Quantum* **2**, 79 (2018), arXiv:1801.00862.

[5] S. Endo, S. C. Benjamin, and Y. Li, *Journal of the Physical Society of Japan* **90**, 032001 (2021).

[6] J. R. McClean, S. Boixo, V. N. Smelyanskiy, R. Babbush, and H. Neven, *Nature Communications* **9**, 4812 (2018).

[7] M. Cerezo, A. Sone, T. Volkoff, L. Cincio, and P. J. Coles, Cost function dependent barren plateaus in shallow quantum neural networks (2021).

[8] M. LaRocca *et al.*, *Quantum* **6**, 824 (2022).

[9] M. Schuld and N. Killoran, *Physical Review Letters* **122**, 040504 (2019).

[10] Y. Liu *et al.*, *Nature Communications* **12**, 692 (2021).

[11] J. Watrous, *The Theory of Quantum Information* (Cambridge University Press, 2018).

[12] H.-Y. Huang, R. Kueng, and J. Preskill, *Nature Physics* **16**, 1050 (2020).

[13] F. Brandão and M. Piani, *Reviews of Modern Physics* **93**, 025002 (2021).

[14] J. Walgate, A. J. Short, L. Hardy, and V. Vedral, *Physical Review Letters* **85**, 4972 (2000).

[15] C. W. Helstrom, *Quantum Detection and Estimation Theory* (Academic Press, 1976).

[16] D. Gottesman, *Stabilizer Codes and Quantum Error Correction*, Ph.D. thesis, California Institute of Technology (1997), arXiv:quant-ph/9705052.

[17] M. A. Nielsen and I. L. Chuang, *Quantum Computation and Quantum Information* (Cambridge University Press, 2000).

[18] A. S. Holevo, *Probabilistic and Statistical Aspects of Quantum Theory*, 2nd ed. (Edizioni della Normale, 2011).

[19] W. Hoeffding, *Journal of the American Statistical Association* **58**, 13 (1963).

[20] S. L. Braunstein and C. M. Caves, *Physical Review Letters* **72**, 3439 (1994).

[21] M. Hayashi, *Quantum Information: An Introduction* (Springer, 2006).

[22] J. Watrous, *The Theory of Quantum Information* (Cambridge University Press, 2018).

[23] W. Matthews, S. Wehner, and A. Winter, *Communications in Mathematical Physics* **291**, 813–843 (2009).

[24] C. Lancien and A. Winter, *Communications in Mathematical Physics* **323**, 555–573 (2013).

[25] W. H. G. Correa, L. Lami, and C. Palazuelos, *IEEE Transactions on Information Theory* **68**, 7306–7314 (2022).

[26] F. A. Mele and L. Lami, Optimising quantum data hiding (2025), arXiv:2510.03538 [quant-ph].

[27] D. Rippchen, M. Sreekumar, and M. Berta, arXiv preprint (2024), arXiv:2405.05037.